Structure/Nuclease Activity Relationships of DNA Cleavers Based on Cationic Metalloporphyrin−Oligonucleotide Conjugates†

Béatrice Mestre, Andreas Jakobs, Geneviève Pratviel, and Bernard Meunier*

Laboratoire de Chimie de Coordination du CNRS, 205 Route de Narbonne, 31077 Toulouse Cedex, France

Received December 22, 1995; Revised Manuscript Received April 1, 1996⊗

ABSTRACT: The covalent attachment of a manganese-tris(methylpyridiniumyl)porphyrin entity to an antisense oligonucleotide allowed sequence-selective oxidative cleavage of DNA when the metalloporphyrin was activated by potassium monopersulfate ($KHSO_5$). We prepared several structurally modified metalloporphyrin−oligonucleotide conjugates in order to find out the most efficient compound for *in vitro* DNA cleavage. The nature and the length of the tether were modulated, the metalloporphyrin entity was modified (metal, ligand), and different ways of activation of the metalloporphyrin were assayed. We noticed that the location of the peptidic bond within the linker could greatly affect the cleavage efficiency of the different conjugates. We showed that the most efficient conjugate for oxidative DNA cleavage was a manganese tetracationic porphyrin−oligonucleotide compound. When the metalloporphyrin moiety was activated by a reducing agent in the presence of molecular oxygen, DNA cleavage was efficient at suitable concentrations of the reducing agent, in order to avoid the reduction of the activated DNA cleaver, a putative high-valent metal−oxo species, by the excess of reducing agent.

Diaquamanganese(III) *meso*-tetrakis(4-*N*-methylpyridiniumyl)porphyrin (Mn-TMPyP)[1] is an efficient artificial endonuclease when associated to $KHSO_5$ as oxygen atom donor (Pitié et al., 1992; Pratviel et al., 1993a). This cationic complex mediates oxidative DNA cleavage *via* an activated form of the metalloporphyrin, namely, a high-valent metal−oxo species (Bernadou et al., 1994; Pitié et al., 1995). This activated species is reminiscent of the activated form of iron−bleomycin (Burger et al., 1995; Guajardo et al., 1995; Pratviel et al., 1989; Sam et al., 1994) or the heme−ferryl species of cytochrome P-450 monooxygenases and related metalloporphyrin enzyme models (McMurry & Groves, 1986; Meunier, 1992) that are generated (*in vivo* for iron−bleomycin and cytochrome P-450) by O_2 and a source of electrons. The mechanism of DNA cleavage of the Mn-TMPyP/$KHSO_5$ system involves an oxidative attack of DNA deoxyribose units as the initial step followed by other steps (e.g., β-eliminations) leading to strand scission. We showed that the high-valent metal−oxo porphyrin complex ("activated form") was able to hydroxylate C−H bonds at C1′ and C5′ of DNA deoxyriboses through a strong interaction of the cationic compound within the minor groove of B-type DNA (Pitié et al., 1992, 1995; Pratviel et al., 1993b).

The high DNA cleavage activity of activated Mn-TMPyP makes cationic manganese porphyrin very attractive as a reactive DNA cleaver to be linked to oligonucleotides for specific DNA cleavage *in vitro* and also for the possible use of these modified oligonucleotides within cells to eliminate integrated viral DNA or to inhibit mRNA translation [for recent articles on oxidative oligonucleotide-cleaver conjugates, see Dervan (1992) and Sigman et al. (1993, and references therein), and for hydrolytic oligonucleotide-cleavers, see Bashkin et al. (1994), Hall et al. (1994), Magda et al. (1994), and Matsumara et al. (1994)]. Preliminary data indicated that single-stranded (Pitié et al., 1993; Pratviel et al., 1995; Mestre et al., 1995) or double-stranded DNA (Bigey et al., 1995) can be cleaved by these cationic metalloporphyrin−oligonucleotide conjugates.

The first cationic metalloporphyrin−oligonucleotide conjugate was designed to target the region containing the initiation codon of the *tat* gene of HIV-1 (compound **1** on Figure 1). The anti-*tat* 19-mer sequence was complementary to the 35-mer *tat* DNA target containing the first eight codons of *tat* gene of HIV-1 [5360−5394 according to Wain-Hobson et al. (1985)]. The 15-bond long linker of conjugate **1** was rather hydrophobic with ten methylene groups, four for the aliphatic carboxylic acid of the metalloporphyrin-arm and six for the 5′-amino-linked oligonucleotide (Casas et al., 1993b). This parent conjugate showed selective DNA cleavage properties *in vitro* when the metalloporphyrin moiety was activated by potassium monopersulfate (Pitié et al., 1993; Mestre et al., 1995).

In order to enhance the cleavage yield and to understand the molecular basis of the reactivity of this oligonucleotide cleaver, we tried several chemical modifications on the structure of this conjugate. Here we report the influence of the modified parameters, namely, (i) length and nature of the linker and (ii) structure of the metalloporphyrin (metal, number of positive charges of ligand), on the cleavage activity against two HIV DNA targets: a 35-mer containing

† This work was supported by ANRS (French Agency for Research on AIDS), ARC (Association pour la Recherche contre le Cancer, Villejuif, France), Région Midi-Pyrénées and CNRS. B. Mestre and A. Jakobs are indebted to the Ministère de l′Enseignement Supérieur et de la Recherche (MESR) and to the European Community (HCM program) for PHD and post-doctoral fellowships, respectively.

⊗ Abstract published in *Advance ACS Abstracts,* June 15, 1996.

[1] Abbreviations: CDI, *N*,*N*′-carbonyldiimidazole; HOBt, 1-hydroxybenzotriazole; BOP, benzotriazol-1-yloxytris(dimethylamino)phosphonium hexafluorophosphate; ds DNA, double-stranded DNA; HEPES, *N*-(2-hydroxyethyl)piperazine-*N*′-(2-ethanesulfonic acid); Mn-TMPyP, pentaacetate of diaquamanganese(III) *meso*-tetrakis(4-*N*-methylpyridiniumyl)porphyrin; MOPS, 3-(*N*-morpholino)propanesulfonic acid; NMM, *N*-methylmorpholine; OD, optical density; ss DNA, single-stranded DNA; TEAA, triethylammonium acetate; TRIS, tris(hydroxymethyl)aminomethane.

S0006-2960(95)03040-6 CCC: $12.00

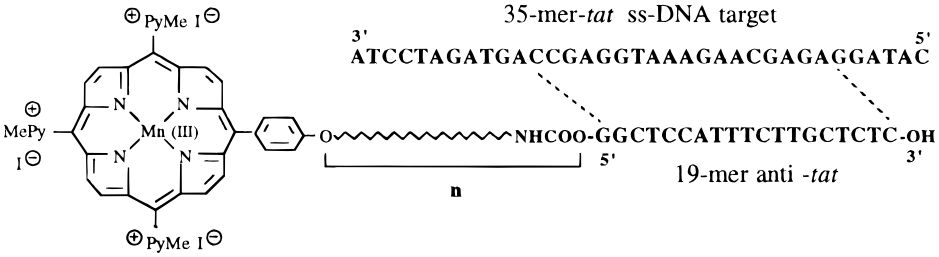

	LINKER	n	X
1	-O-$(CH_2)_4$-CONH-$(CH_2)_6$-NHCOO-	15	80 %
2	-O-CH_2-CONH-$(CH_2)_6$-NHCOO-	12	90 %
3	-O-CH_2-CONH-$(CH_2)_2$-NHCOO-	8	50 %
4	-O-$(CH_2)_4$-CONH-$(CH_2)_2$-NHCOO-	11	50 %
5	-O$(CH_2)_4$-CONH-$(CH_2)_3$-NH-$(CH_2)_4$-NH-$(CH_2)_3$-NHCOO- (spermine)	21	60 %

FIGURE 1: Structures of anti-*tat* conjugates: variation of length and nature of the linker. The number of bonds **n** was calculated as number of single bonds between the phenoxy oxygen atom of the porphyrin precursor and the 5′-oxygen atom of the antisense oligonucleotide. **X** is the yield of target DNA cleavage, after piperidine treatment (see Figure 3).

the initiation codon of *tat* and a 35-mer containing the initiation site of *rev* [5507−5541 according to Wain-Hobson et al. (1985)] which is highly conserved in different viral isolates (Matsukara et al., 1987, 1991). We also tried two different ways of activation of the metalloporphyrin cleaver. In one series of DNA cleavage experiments the active metal−oxo species was classically generated by addition of $KHSO_5$, and in the second series the metalloporphyrin entity was activated in the presence of O_2 and a reducing agent, as should occur *in vivo* for bleomycin mimics that are linked to antisense oligonucleotides.

In the present article, we report that the nature and the length of tether as well as the position of the amide bond within the linker greatly affected the cleavage efficiency of the different conjugates. The number of positive charges of the metalloporphyrin entity had also a strong influence on the cleavage efficiency of these metalloporphyrin−oligonucleotide conjugates. The tethered tetrapyridiniumyl metalloporphyrin was a better DNA cleaver than trispyridiniumyl ones. We have also found suitable conditions for the reductive activation of the manganese porphyrin−oligonucleotide conjugates by reducing agent in the presence of molecular oxygen leading to DNA breaks in a bleomycin-like fashion.

EXPERIMENTAL PROCEDURES

Synthesis, Purification, and Labeling of Oligonucleotides. All oligodeoxynucleotides (19-mer anti-*tat*, 26-mer anti-*rev*, and 35-mer *tat* and *rev* targets) were synthesized by standard solid phase β-cyanoethyl phosphoramidite chemistry on a Cyclone Plus DNA synthesizer from Milligen-Biosearch. 5′-Hexamethylenediamine-, -ethylenediamine-, and -spermine-modified oligonucleotides were obtained by using the method previously described to functionalize the 5′-end of oligonucleotides by diamines (Wachter et al., 1986).

5′-NH_2-oligonucleotides were purified by HPLC using a reverse-phase C18 column [Nucleosil C18, 10 μM from Interchrom; eluents, A = 0.1 M triethylammonium acetate (TEAA) (pH 6.5), B = CH_3CN; linear gradient, 10−30% B over 45 min; flow rate, 1 mL/min; λ = 260 nm]. Purification of both 35-mer *tat* and *rev* targets was performed by electrophoresis on 20% polyacrylamide denaturing gels. Concentrations of ss oligonucleotides were determined by UV measurements at 260 nm.

The 5′-end of the two 35-mer targets was labeled by [^{32}P] using standard procedures with T_4 polynucleotide kinase and [γ-^{32}P]ATP purchased from Biolabs and from Dupont, respectively.

Preparation of Metalloporphyrin Precursors. All metalloporphyrin precursors were prepared in our group by total synthesis starting from pyrrole and modified aldehyde derivatives. The metalloporphyrin moiety of conjugates **1**, **4**, **5**, and **6**, namely, manganese(III) 5-[(4-(5-carboxy-1-butoxy)phenyl]-10,15,20-tris(4-*N*-methylpyridiniumyl)-porphyrin, was prepared according to Casas et al. (1993a). Manganese(III) 5-[(4-(2-carboxy-1-methoxy)phenyl]-10,15,20-tris(4-*N*-methylpyridiniumyl)porphyrin precursor of conjugates **2** and **3** and the iron(III) 5-[(4-(5-carboxy-1-butoxy)-phenyl]-10,15,20-tris(4-*N*-methylpyridiniumyl)porphyrin precursor of **8** were prepared as described (Bigey et al., 1996). The new tetracationic metalloporphyrin cleaver entity of conjugate **7**, namely manganese(III) 5-[4-*N*-(4-carboxy-1-butyl)pyridiniumyl]-10,15,20-tris(4-*N*-methyl-pyridiniumyl)porphyrin, was prepared by monoalkylation of the commercially available symmetrical tetrapyridylporphyrin with 5-bromopentanoic ethyl ester (Jakobs et al., submitted). All porphyrin precursors were metalated by $MnCl_2$ or $(NH_4)_2$-$Fe(SO_4)_2$ before they were coupled to the desired oligonucleotide. Consequently all these water-soluble metalloporphyrin conjugates have two water molecules on the axial positions of the metal center and an additional positive charge (these ligands and the extra charge were omitted from Figures 1 and 2 for clarity).

Preparation of Metalloporphyrin−Oligonucleotide Conjugates. The hybrid "metalloporphyrin−oligonucleotide" molecules **1**−**8** (see Figures 1 and 2 for structures) were

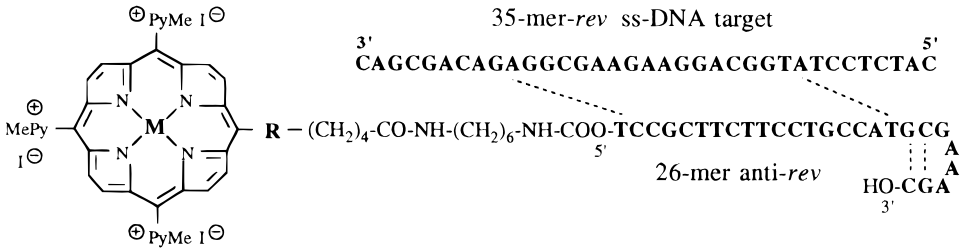

	R	M
6	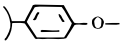	Mn(III)
7	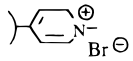	Mn(III)
8	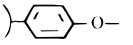	Fe(III)

FIGURE 2: Structures of anti-*rev* conjugates: metalloporphyrin modifications.

synthesized according to the methods described below through the formation of a peptidic link between the 5′-NH_2 end of oligonucleotides and the carboxylate terminal group of metalloporphyrin precursors. The anionic counter-ions of the metalloporphyrin precursors (iodide, chloride, and/or bromide) were not exchanged for acetate ions to avoid the activation of this latter carboxylic counter-ion with the peptide chemistry used to prepare the different conjugates. Progress of coupling reactions was followed by liquid chromatography using an anion exchange column [Protein Pak DEAE 8 HR from Waters, 8 cm × 1 cm; A = 25 mM TRIS/HCl (pH 8.5), B = A + 1 M NaCl; linear gradient, 20−50% B over 45 min; flow rate, 0.7 mL/min]. Resulting conjugates were purified by liquid chromatography in the same conditions and desalted on Sep-Pak cartridges from Waters. During chromatographic analyses, profiles were monitored by a two-channel diode array detector 440 from Kontron (λ = 260 nm and 468 nm or 430 nm for manganese(III) or iron(III) porphyrins, respectively), which also allowed the yield of coupling reactions to be estimated by comparing the conjugate products with the starting 5′-NH_2 modified oligonucleotides. Typically, yields of purification of conjugates ranged from 80% to 90% according to the amount of conjugate estimated by liquid chromatography after the coupling reaction.

*Synthesis of **1**, **5**, and **6**.* These conjugates were synthesized according to a method already described (Mestre et al., 1995) involving an activation of the carboxylic function by *N*,*N*′-carbonylimidazole (CDI) and hydroxybenzotriazole (HOBt) of the manganese porphyrin precursor and a coupling step with the 5′-hexamethylenediamine-19-mer anti-*tat* for conjugate **1**, the 5′-spermine-19-mer anti-*tat* for **5**, and the 5′-hexamethylenediamine-26-mer anti-*rev* for **6**. Yields of coupling reactions were 60% for conjugates **1** and **6** and 70% for **5**.

*Synthesis of **2**−**4**.* To 108 μL of a 1.5 mM solution of the corresponding manganese tris(methylpyridiniumyl)-porphyrin precursor (0.16 μmol) with a 4-(2-carboxy-1-methoxy)phenyl tether for conjugates **2** and **3** or a 4-(5-carboxy-1-butoxy)phenyl linker for **4**, in dry DMF (DMF was dried over barium oxide, distilled, and kept over 4 Å molecular sieves) were added 0.5 μL of *N*-methylmorpholine (NMM) (4.7 μmol) and 25 μL of two 63.2 mM solutions of benzotriazol-1-yloxytris(dimethylamino)phosphonium (BOP) and HOBt (1.58 μmol of each coupling agents) in dry DMF. After 15 min at 60 °C, the solutions of benzotriazole-activated esters were added to the corresponding 5′-NH_2-substituted oligonucleotide: 5′-hexamethylenediamine-19-mer anti-*tat* for conjugate **2** or 5′-ethylenediamine-19-mer anti-*tat* for **3** and **4** (31.3 nmol, 5 OD_{260} units) in 158 μL of 20 mM MOPS buffer (pH 7.5). The coupling reaction medium consisted of a 50/50 mixture of 20 mM MOPS buffer with DMF (v/v). Solutions were incubated at 37 °C for 1 h, then 500 μL of methanol was added and the medium was centrifuged. After removal of the supernatant, the pellet was washed with methanol (2 × 500 μL) and dried under vacuum (Speedvac from Bioblock). This precipitation procedure was also used for conjugates **7** and **8** described below. Conversion of the starting oligonucleotides to conjugates was 40% for products **2** and **4** and only 10% for **3** despite several attempts.

*Synthesis of **7**.* The procedure described above was modified for the preparation of **7**. The same amount of oligonucleotide, 5′-hexamethylenediamine-26-mer anti-*rev* (31.3 nmol, 7.2 OD_{260} units) was dissolved in 63 μL of 20 mM MOPS buffer (pH 7.5), and the activated ester was prepared in 253 μL of dry DMF with 0.8 μmol (150 μL of a 5.3 mM solution) of manganese tetracationic precursor, 27 μmol (3 μL) of NMM and 7.9 μmol (50 μL of 0.16 M solutions) of BOP and HOBt. The coupling reaction was performed in a 20/80 mixture of 20 mM MOPS buffer (pH 7.5) and DMF during 1 h at 50 °C. Isolation and purification steps were as indicated above (coupling reaction yield = 30%).

*Synthesis of **8**.* The iron(III) 5-[(4-(5-carboxy-1-butoxy)-phenyl]-10,15,20-tris(4-*N*-methylpyridiniumyl)porphyrin precursor (1 mg, 0.8 μmol) was dissolved in 30 μL of dry DMF followed by the addition of 3 μL of 1-methylimidazole (38 μmol) and 15 μL of 0.75 M solution of CDI in DMF (11.2 μmol). Formation of the imidazolide was allowed to take place over 2 h at room temperature, then 15 μL of a 0.59 M solution of HOBt in dry DMF (8.8 μmol) was added, and after 2 h, the excess of CDI was quenched by addition of 20 μL of 20 mM MOPS buffer (pH 7.5). After 15 min, the

activated ester was added to the 5′-hexamethylenediamine-26-mer anti-*rev* (31.3 nmol, 7.2 OD_{260} units) dissolved in 233 μL of 20 mM MOPS buffer (pH 7.5). The coupling of both reagents was performed in an 80/20 mixture of 20 mM MOPS buffer and DMF. The mixture was heated at 60 °C for 12 h, and the coupling product was precipitated by addition of 500 μL of methanol. After centrifugation of the medium, the supernatant was removed, and the pellet was washed with methanol (2 × 500 μL) and taken up in 200 μL of 0.3 M sodium acetate buffer (pH 5.2), followed by precipitation with 600 μL of ethanol overnight at −20 °C. Coupling reaction yield was 70%.

Spectrophotometric and Liquid Chromatography Data Relative to Oligonucleotides, Metalloporphyrins, and Conjugates. ϵ_{260} values of oligonucleotides in water: 5′-OH or 5′-NH_2-19-mer anti-*tat* = 160×10^3 M^{-1} cm^{-1}, 5′-OH or 5′-NH_2-26-mer anti-*rev* = 230×10^3 M^{-1} cm^{-1}. ϵ values of metalloporphyrin precursors in methanol: ϵ_{468} of manganese(III) porphyrin derivatives = 100×10^3 M^{-1} cm^{-1}; ϵ_{430} of iron(III) porphyrin derivative = 90×10^3 M^{-1} cm^{-1}. For hybrid molecules, the observed visible/UV ratios monitored by diode array detector spectra of liquid chromatography conjugate peaks were as follows: A_{468}/A_{260} for **1** = 0.65, **2** = 0.65, **3** = 0.72, **4** = 0.71, **5** = 0.57, **6** = 0.47, and **7** = 0.74; A_{430}/A_{260} for **8** = 0.50. The retention times of oligonucleotides and conjugates analyzed by liquid chromatography on an anion exchange chromatography (Protein Pak) were as follows: 26 min for 5′-hexamethylenediamine and 5′-ethylenediamine-19-mer anti-*tat*, 24 min for 5′-spermine-19-mer anti-*tat*, 32 min for 5′-hexamethylenediamine-26-mer anti-*rev*, 22 min for **1**−**4**, 20 min for **5**, 29 min for **6** and **8**, and 28 min for **7**. Concentrations of conjugate solutions were determined spectrophotometrically at 260 nm as for ss oligonucleotides.

DNA Cleavage Reactions. DNA cleavage reactions (final reaction volume = 16 μL) were performed with 5′-labeled 35-mer *tat* or *rev* as ss DNA target [final concentration 10 nM; (10−20) × 10^3 cpm] and the corresponding conjugates **1**−**8** (final concentration 10 nM, target to conjugate ratio = 1/1) in the presence of an excess of random herring testes double-stranded DNA (0.4 mM in nucleotides, 880 equiv with respect to the target) in 100 mM NaCl, 50 mM phosphate buffer (pH 7). Annealing of conjugates with complementary 35-mer was achieved by heating at 90 °C for 1 min followed by slow cooling to 25 °C. For control reactions carried out without any cleaving agent, the 19-mer anti-*tat* and 26-mer anti-*rev* were hybridized with their complementary 35-mer target. DNA cleavage reactions were initiated by adding 1 μL of a freshly prepared solution of $KHSO_5$ (final concentration from 1 μM to 1 mM) or dithiothreitol (DTT; final concentration from 10 nM to 10 mM). When the activation of the metalloporphyrin entity was performed with $KHSO_5$, the DNA cleavage reaction lasted 1 h at 4 °C (unless specified otherwise in the text) and was stopped by the addition of 1 μL of 1 M Hepes (pH 8). But when the metal complex was activated by a reducing agent and molecular oxygen, the DNA cleavage reaction was allowed to proceed for 15 h at 37 °C and stopped by ethanol precipitation as indicated below. Piperidine treatments performed in some cases on DNA cleavage products consisted of a thermal step at 90 °C during 1 h in the presence of 1 M piperidine. Samples were then diluted with 20 μL of 0.3 M sodium acetate buffer (pH 5.2) containing yeast tRNA at 0.1 mg/mL, precipitated with 200 μL of cold ethanol overnight at −20 °C. After centrifugation (10 min at 4 °C, 12 × 10^3 rpm), the DNA pellet was washed with cold 90% ethanol, dried under vacuum (Speedvac), and dissolved in formamide with marker dyes. DNA fragments were subjected to electrophoresis on denaturing (7 M urea) 20% polyacrylamide gel (3 h at 2300 V).

RESULTS

The DNA cleavage activity of the different metalloporphyrin−oligonucleotide conjugates was asseyed *in vitro* toward two different ss DNA target sequences: a 35-mer *tat* and a 35-mer *rev* corresponding to the initiation sites of *tat* and *rev* HIV-1 genes, respectively. Two series of different metalloporphyrin−oligonucleotide conjugates carrying the complementary anti-*tat* or anti-*rev* oligonucleotide were designed (see Figures 1 and 2 for anti-*tat* and anti-*rev* conjugates, respectively). The influence of the length and nature of the tether on conjugate reactivity was studied with the anti-*tat* series, whereas the influence of the number of cationic charges on the porphyrin ligand and the difference of reactivity of the metal center was studied with the anti-*rev* family of conjugates. The comparison between two different ways of activation (peroxide versus molecular oxygen and electrons) of the metalloporphyrin was undertaken with the parent conjugate **6** of the anti-*rev* family and its iron analogue **8**. In each series, the parent conjugate was present (**1** in the anti-*tat* series, Figure 1, **6** in the anti-*rev* series, Figure 2) so that we could evaluate a sequence effect, if any.

In the anti-*rev* series the complementary 18-mer oligonucleotide was lengthened by an 8-nucleotide long sequence that forms a stable miniloop at the 3′-end of the oligonucleotide. This very stable miniloop protects oligonucleotides from 3′-exonuclease degradation (Hirao et al., 1992, 1994; Khan et al., 1993; Poddevin et al., 1994). In the anti-*tat* conjugate series, this 3′-loop was absent. But we have shown previously that the parent conjugate **1** elongated with the same 3′-miniloop had the same cleavage pattern than that of the reagent without 3′-loop with only a slight decrease of the cleaving efficiency by a factor of 2 (Mestre et al., 1995).

Influence of Length and Nature of Linker on Nuclease Activity of Conjugates. The comparison of the nuclease activity of metalloporphyrin−oligonucleotide conjugates as a function of the linker length was performed with compounds **1**−**4**. Because we expected that the electrostatic positive effect of a spermine molecule (Schmid et al., 1991; Bigey et al., 1995) at physiological pH would allow a better fitting of the linker with DNA and consequently an increased cleaving activity of the metalloporphyrin−oligonucleotide conjugate, compound **5** was prepared. Comparative DNA cleavage experiments were performed with the 5′-labeled 35-mer *tat* at a final concentration of 10 nM which was incubated in the presence of 10 nM of conjugate (only one molecule of cleaver for one DNA target) with an excess of random ds DNA and are presented in Figure 3. Initiation of the cleavage reaction was achieved by addition of $KHSO_5$ (final concentration of 1 mM), and the cleavage reaction time was 1 h at 4 °C. Piperidine treatments were performed to reveal all damages mediated by conjugates on their DNA target (direct cleavage and base damages). As previously

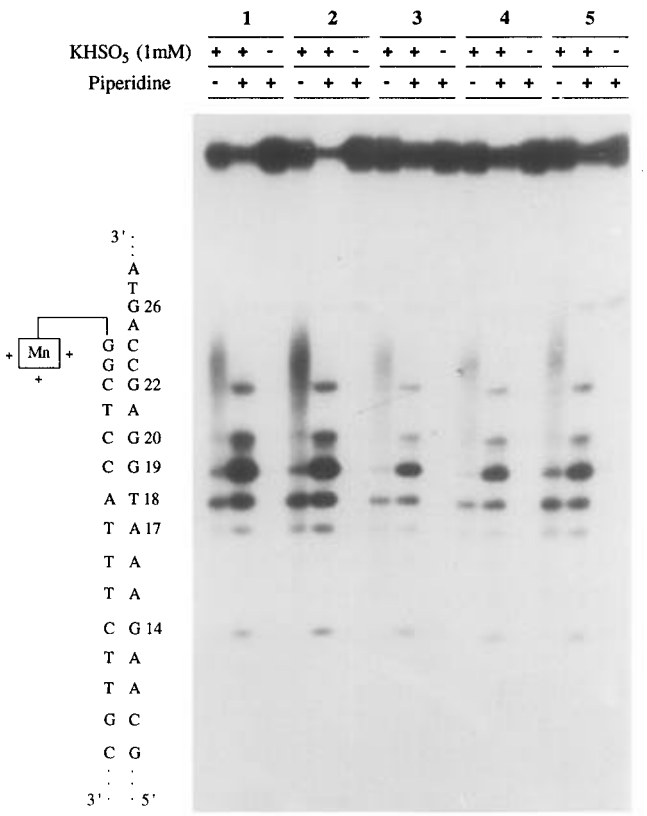

FIGURE 3: Influence of the linker in the anti-*tat* conjugates series. All of the compounds consisted of a manganese trispyridiniumylporphyrin entity coupled to the anti-*tat* 19-mer *via* aliphatic diamine linker or spermine. Cleavage of 5′-[^{32}P]-35-mer *tat* ss DNA target with conjugates **1**−**5**. The target-labeled DNA and conjugates were 10 nM each, excess random ds DNA was 0.4 mM base. The cleavage reaction proceeded for 1 h at 4 °C in the presence of 1 mM of $KHSO_5$ in 100 mM NaCl, 50 mM phosphate buffer (pH 7). Cleavage reactions were analyzed before and after piperidine treatment as indicated on the top of the gel.

reported (Mestre et al., 1995), DNA cleavage by conjugate **1** consisted of a smear reaching from G_{20} to G_{26} (Maxam and Gilbert positions) and two main individual bands at G_{19} and T_{18} before piperidine treatment (Figure 3, lane 1). These smears are due to multiple modes of oxidative cleavage events (Mestre et al., 1995). After alkaline treatment, the smear and a part of the full-length material were transformed to bands corresponding mainly to G_{19} damages and to some lower extent to G_{20}, G_{22}, and also G_{26}, while band intensities corresponding to T_{18} only slightly increased (Figure 3, lane 2). Direct breaks at T_{18} and G_{19} might correspond to sugar oxidation as described for Mn-TMPyP (Pitié et al., 1992), whereas piperidine treatment revealed guanine oxidation damages. On the G_{19} residue the two mechanisms of cleavage occurred. This particular point on guanine oxidations will be also discussed later in the case of the 35-mer *rev* target sequence.

Conjugates **2**−**5** led to similar patterns of cleavage, but they presented quite different efficiencies of cleavage of the 35-mer *tat* target. According to densitometric analyses, degradation of the 35-mer *tat* was 80% for the parent compound **1** (lane 2) and 90% for **2** (lane 5), each having a 15- and 12-bond linker, respectively. When the linker lengths were further reduced to 11 and 8 bonds, the yield of cleavage decreased to 50% for both conjugates **3** (lane 8) and **4** (lane 11). For the spermine-containing conjugate **5**, the cleavage yield was 60% (lane 14). But for compound **5**, the amount of damage due to direct breaks at G_{19} and T_{18} compared to piperidine-sensitive lesions was higher than for conjugate **1**. Before piperidine treatment (compare lane 1 with **1** and lane 13 with **5**) the same amount of direct cleavage occurred, whereas after alkaline treatment compound **1** was much more efficient in G oxidation (compare lane 2 with **1** and lane 14 with **5**).

Influence of Number of Positive Charges of the Porphyrin Ligand on Nuclease Activity of Metalloporphyrin−*Oligonucleotide Conjugates.* This effect was studied with conjugates **6** and **7** presented in Figure 2. Compared to conjugate **6** based on the classical tris(methylpyridiniumyl)-porphyrin ligand with three positive charges on the porphyrin ligand used for all conjugates of the anti-*tat* series (Figure 1), compound **7** exhibits four positive charges on the porphyrin macrocycle. This complex might have a higher DNA affinity and consequently a better DNA cleavage activity.

The cleavage of the 5′-[^{32}P]-labeled 35-mer *rev* target by the parent compound **6** is illustrated in Figure 4. The 35-mer *rev* target (final concentration 10 nM) was incubated in the presence of a final concentration of 10 nM of conjugate **6** (1 equiv with respect to the target) and a large excess of random ds DNA. The oxidative cleavage of DNA was initiated by addition of a $KHSO_5$ solution (final concentration of 1 or 0.1 mM, as indicated on Figure 4). As mentioned before, some oxidative lesions mediated by conjugates **6** and **7** on the DNA target were not revealed without piperidine treatment. Before piperidine treatment the pattern of cleavage of compound **6** with 1 mM $KHSO_5$ (Figure 4) consisted, as also observed in the anti-*tat* series, of a smear from the 35-mer full-length band to a fragment corresponding to the G_{22} band of the Maxam−Gilbert ladder. After alkaline treatment, cleavage fragments mediated by compound **6** activated by 1 mM $KHSO_5$, appeared as discrete bands corresponding to G_{22} and G_{24} fragments of the Maxam−Gilbert ladder as major bands and to G_{19}, G_{25}, and G_{27} fragments as minor ones (Figure 4). Densitometric evaluation of cleaving efficiency of conjugate **6** indicate that 75% of the 35-mer *rev* target was damaged with only 1 equiv of DNA cleaver with respect to the target and 1 mM of monopersulfate. When the concentration of $KHSO_5$ was decreased to 0.1 mM, the overall cleavage yield decreased to 50% of degradation of target after piperidine treatment (Figure 4). The main site of cleavage was then located at the G_{27}, i.e., at the junction of single- and double-stranded regions of the DNA target.

The reactivity of the conjugate **7** is illustrated in the same Figure 4. In the presence of 1 mM of $KHSO_5$, and after piperidine treatment, damages on the 35-mer were estimated to be 75%, as for conjugate **6**, but the cleavage profile by **7** was different than that obtained with **6**. The major fragment generated by **7** was located at G_{22} with minor fragments at G_{19}, A_{21}, and G_{24}. The metalloporphyrin cleavage sites seemed to be located mainly in the double-stranded region generated by the hybridization of the oligonucleotide vector of the cleaver onto the 35-mer target. When the cleavage of **7** and **6** was compared at lower concentration of $KHSO_5$ (0.1 mM), the DNA cleavage products of **7** were also shorter than those obtained with **6**, and they were mainly located in the duplex region. Densitometric titration of the remaining intact 35-mer *rev* material showed that, for 0.1 mM of $KHSO_5$, the cleavage yield of the tetracationic porphyrin

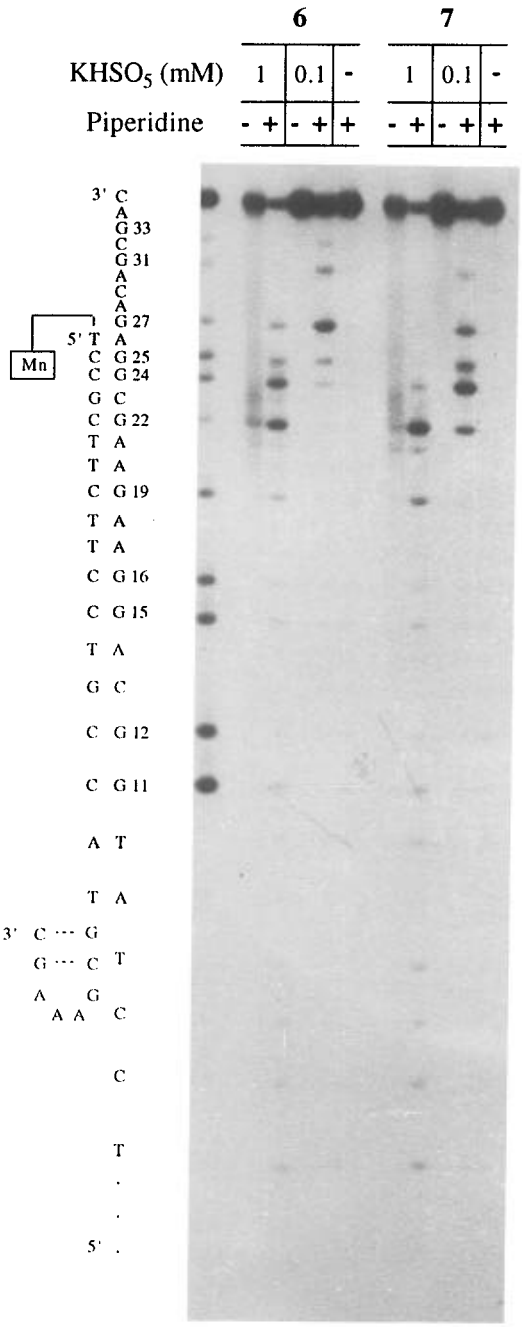

FIGURE 4: Variation of Mn−porphyrin structure in the conjugates of the anti-*rev* family. Cleavage of 5′-[^{32}P]-35-mer *rev* ss DNA target (10 nM) with the parent tricationic porphyrin conjugate **6** (10 nM) (lanes 1−5) and the tetracationic porphyrin conjugate **7** (10 nM) (lanes 6−10) in the presence of 0.1 or 1 mM $KHSO_5$ concentrations. The cleavage reaction was in 100 mM NaCl, 50 mM phosphate buffer (pH 7) for 1 h at 4 °C. For each compound and at each concentration of $KHSO_5$, DNA cleavage was analyzed before and after piperidine treatment as indicated at the top of the gel. Maxam and Gilbert G reaction is presented in the first lane on the left of the gel.

conjugate **7** was 60%, slightly higher than that obtained with the tricationic porphyrin conjugate **6** (50% of cleavage). This difference can be explained by a higher reactivity of the tetracationic metalloporphyrin entity as also deduced from experiments described on Figure 5 where cleavage reactions with **6** and **7** were performed at various concentrations of $KHSO_5$ ranging from 1 mM to 1 μM (from left to right on Figure 5). Only the cleavage patterns after piperidine treatment were compared. For compound **6**, at 1 and 10

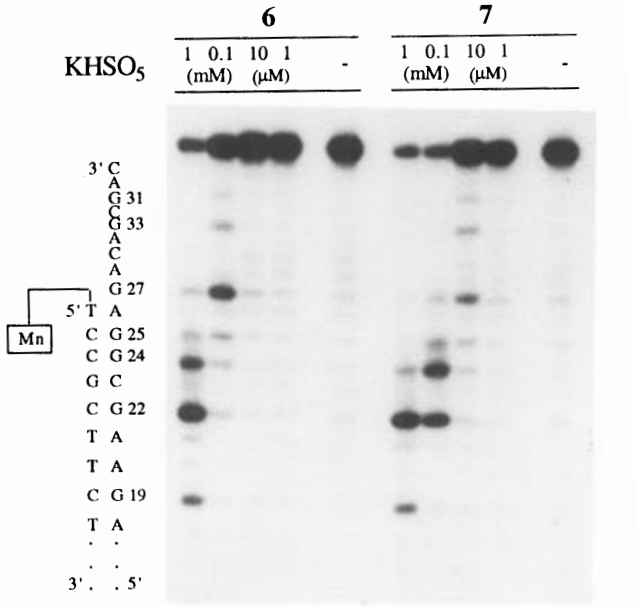

FIGURE 5: Variation of the concentration of $KHSO_5$. Cleavage of 5′-[^{32}P]-35-mer *rev* ss DNA target with the tricationic (**6**) or tetracationic (**7**) conjugates (lanes 1−5 or 6−10, respectively) analyzed only after piperidine treatment. The target labeled 35-mer *rev* (10 nM) was incubated in the presence of the conjugate (10 nM) and an excess of random ds DNA in 100 mM NaCl, 50 mM phosphate buffer (pH 7) with $KHSO_5$ for 1 h at 4 °C. $KHSO_5$ concentrations were decreased from left to right on the figure: 1 mM, 100 μM, 10 μM, 1 μM, or none for each conjugate.

μM of $KHSO_5$ no degradation of the target was observed (Figure 5, lane 3 and 4). For 100 μM of oxidant, the cleavage pattern consisted of fragments due to damages mainly located in the ss region at G_{27} (Figure 5, lane 2). At 1 mM of $KHSO_5$ (Figure 5, lane 1) major cleavage fragments were mediated in the ds zone of the cleaver−target duplex, as previously described in Figure 4. The G_{27} guanine of 35-mer *rev* was thus probably the nearest and first guanine base to be attacked by the activated metalloporphyrin. In the presence of higher concentration of $KHSO_5$ secondary cleavage events on this G_{27} ending fragment led to products cleaved at G_{24} and G_{22}. The same cleavage profile was also observed for conjugate **7**, the first cleavage event taking place in the ss region at G_{27} position. But, for compound **7**, the same DNA break profiles were obtained with $KHSO_5$ concentrations 1 order of magnitude lower than for conjugate **6** (DNA cleavage started at 10 μM of $KHSO_5$ with **7**, see lane 8 of Figure 5). Patterns of DNA cleavage for **7** with 100 and 10 μM of $KHSO_5$ (Figure 5, lanes 7 and 8, respectively) were nearly identical to those obtained with **6** with 1 mM and 100 μM of $KHSO_5$ (Figure 5, lanes 2 and 3, respectively). In order to check that the $KHSO_5$ concentration did not affect the binding of the cleaving entity on its target, a reaction time course was performed (data not shown). Reactions with compound **6** were carried out in standard conditions by addition of $KHSO_5$ at a final concentration of 1 mM and at various time intervals (30 s, 3, 5, 12, 20, and 30 min, and 1 h), reactions being stopped by addition of 1 M HEPES (1 μL). After piperidine treatment, cleavage patterns were compared with the ones of Figure 5. After 30 s of reaction, the cleavage profile was identical to that observed with addition of $KHSO_5$ at a final concentration of 0.1 mM (lane 2, Figure 5). Between 30 s and 20 min, the amount of shortoligonucleotide fragments increased up to the profile obtained generally after 1 h of

reaction at 4 °C and with a final concentration of $KHSO_5$ of 1 mM (lane 1, Figure 5). So these short fragments arose from secondary cleavage events. Some faint cleavage observed all the way down to the bottom of some gels, especially on Figure 4 (lanes 2 and 7), was due to $KHSO_5$ itself plus piperidine treatment. As a control experiment, the ss 35-mer *rev* target was annealed with the unconjugated 26-mer anti-*rev* and treated with $KHSO_5$ at a final concentration of 1 mM. After piperidine treatment, the 35-mer *rev* target was slightly degraded especially at guanine residues and along all of the sequence as previously observed on Figure 4.

These results clearly indicate that the metalloporphyrin entities of conjugates **6** and **7** can promote at least two ss DNA breaks when the initial cleaver/target ratio is only 1/1, and thus they behave as catalysts.

Influence of the Nature of the Metal Center and of the Activation Mode of the Metalloporphyrin. Non-conjugated metalloporphyrins have a lower DNA cleavage efficiency when they are activated by a reducing agent in the presence of dioxygen from air compared to monopersulfate activation (Ward et al., 1986). However we decided to compare the nuclease activity of the manganese porphyrin conjugate **6** with the corresponding iron conjugate **8** with two different modes of activation of the metal center. The first one was the generation of a metal−oxo entity by $KHSO_5$, the other one was the mimic of the possible *in vivo* activation of metalloporphyrins in the presence of molecular oxygen and a reducing agent (we tested ascorbate, dithiothreitol, and glutathione). These comparative studies on the role of the metal center and the two different activation modes were performed with the 35-mer *rev* target. Lanes 1−4 of Figure 6 correspond to the manganese porphyrin **6**, and lanes 5−8 correspond to the iron analogue **8**.

$KHSO_5$ activation (at 1 mM concentration) of manganese (lanes 1 and 2) and iron (lanes 5 and 6) porphyrins was analyzed before and after piperidine treatment. Without piperidine treatment the cleavage pattern obtained for compound **8** was a smear of weak intensity extending between the full-size 35-mer band and the G_{24} fragment of the Maxam−Gilbert ladder. Alkaline treatment revealed that the main target damages occurred within the target−oligonucleotide duplex at G residues located at 15, 16, 19 and 22. The cleavage yield for this iron derivative activated by monopersulfate was 50%, which is below that obtained with the corresponding manganese conjugate (75% with **6**), and the attack sites were also different, inside of the duplex rather than at the duplex junction. But, this time, cleavage with **8** in the ds region of target DNA occurred at relatively low cleavage stage (Figure 6), i.e., even at lower concentrations of $KHSO_5$ (10 or 100 μM) (not shown). So it appeared that the iron porphyrin did not interact as the manganese one on the target: an interaction in the ds zone seemed favored for the iron porphyrin.

The activation of manganese porphyrin moiety of conjugate **6** in the presence of air and 0.1 mM of a reducing agent (DTT) was also possible and led to a cleavage pattern identical to that obtained in the $KHSO_5$ activation mode. Compare lane 4 of Figure 6 for O_2 and reductant with lane 2 of Figure 5 for $KHSO_5$ activation at the same concentration of added cofactor (the $KHSO_5$ cleavage reaction was performed at 4 °C during 1 h while the O_2−reductant mode of activation required 12 h at 37 °C). The same pattern of

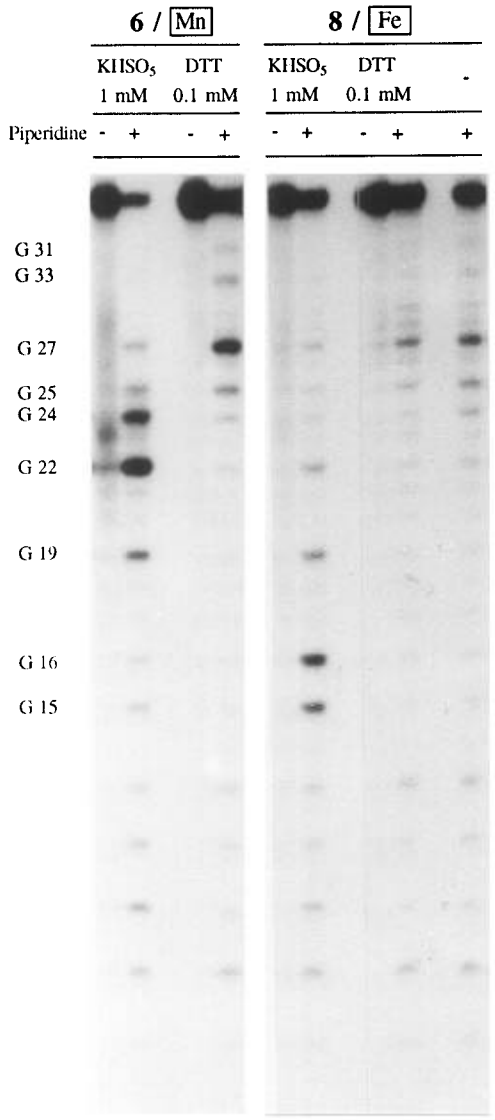

FIGURE 6: Manganese versus iron porphyrin−oligonucleotide conjugates. Comparison of $KHSO_5$ or O_2 and a reductant as activating mode of the Mn-conjugate **6** and its iron analogue **8**. The 5′-[^{32}P]-35-mer *rev* ss DNA target and the conjugate were 10 nM each in 100 mM NaCl, 50 mM phosphate (pH 7) cleavage reaction buffer. They were diluted in a large excess of ds DNA. Activation of metalloporphyrin conjugates by $KHSO_5$ took place at a concentration of 1 mM of $KHSO_5$ and lasted 1 h at 4 °C: lanes 1 and 2 for **6**, and lanes 5 and 6 for **8**. Each pair of lanes correspond to the analysis of the 35-mer *rev* degradation before and after piperidine treatment, repectively. Aerobic activation of the metalloporphyrin−oligonucleotide conjugates in the presence of 0.1 mM of DTT took place over 12 h at 37 °C. The cleavage reactivity of **6** in a reducing medium is illustrated by lanes 3 and 4, before and after piperidine treatment, respectively. The corresponding lanes for compound **8** are lanes 7 and 8. The control of the 35-mer *rev* incubated with **8** without added reducing agent is presented in lane 9.

cleavage was also obtained with glutathione (data not shown). However the degradation yields with conjugate **6** were lower with glutathione, 30% and 60% for 0.1 mM of glutathione and DTT, respectively.

We also observed that the cleavage efficiency of **6** in the presence of O_2 and a reductant was highly dependent on the reductant concentration. Usually, 10 mM or 1 mM concentrations of reducing agents are used for metalloporphyrin-mediated DNA cleavage (Ward et al., 1986). In our case the DNA cleavage was totally inhibited in these conditions.

Various reducing agent concentrations were tested: 10 mM, 0.1 mM, 1 μM, and 10 nM (data not shown). Conjugate **6** cleaved the target only at 0.1 mM of DTT or glutathione according to the profile described above (Figure 6, lane 4). Ascorbate was unable to activate **6** at any concentration. For the iron compound **8**, we never obtained significant DNA breaks in the presence of any reducing agent (Figure 6, lanes 7−9) or in any other experimental conditions by changing the reaction time and/or the temperature.

We also checked that the oxidative DNA lesions mediated by the manganese compound **6** or the iron compound **8**, both being activated by $KHSO_5$, or by **6** activated by DTT were not sensitive to reductants. Addition of a large excess of DTT (10 mM) in each of the above described cleavage reactions before piperidine treatment did not decrease the amount of alkali-labile lesions revealed by piperidine (data not shown).

Sequence Effect on the Nature of DNA Damages Generated by Metalloporphyrin−Oligonucleotide Conjugates. A sequence effect was noted in the nature of the oxidative damages mediated by the metalloporphyrin−oligonucleotide conjugates but not on their overall efficiency of degradation of DNA target. Conjugates **1** and **6** had nearly the same cleaving efficiency on their respective 35-mer ss DNA targets when compared in the same experimental conditions (75%−80% of degradation of DNA target). Conjugate **6** is highly efficient despite of a 3′-mini loop that is known to slightly decrease the cleavage efficiency (Mestre et al., 1995). All DNA breaks mediated by **6** activated by $KHSO_5$ on the 35-mer *rev* sequence were due to guanine oxidation and were revealed after piperidine treatment, whereas we observed two different mechanism for the oxidative damages on the 35-mer *tat* target with the anti-*tat* conjugate **1**: direct single-strand breaks by deoxyribose oxidation and alkali-induced cleavage due to guanine oxydation. This is related to the fact that the *rev* target is G- and C-rich in opposition to the *tat* target sequence that has an A- and T-rich region accessible to the activated metalloporphyrin moiety and leading to damages *via* hydroxylation of C−H bonds at C5′ of deoxyribose units (Pitié et al., 1992; Pratviel et al., 1993).

DISCUSSION

To improve and to better understand the nuclease activity of cationic metalloporphyrin−oligonucleotide conjugates we modified several parameters of these conjugates: (i) the length and the nature of the linker, (ii) the number of positive charges of the porphyrin ligand, and (iii) the metal center and the mode of activation of the metalloporphyrin entity. It must be noted that *the molar ratio of cleaver/target was only 1/1 for all the reported experiments at a final concentration of 10 nM*.

Influence of Length and Nature of the Linker on Nuclease Activity of Conjugates. From data obtained with conjugates **1**−**4**, it is clear that the common feature for the two efficient cleavers **1** and **2** (cleavage yield, 80% and 90%, respectively) was not only the presence of the longest possible linker (n = 15 and 12, respectively) but the necessity of a long tether between the 5′-end of the oligonucleotide vector and the rather rigid peptidic link. Conjugate **4** with only two methylene groups between the 5′-NH-COO-oligonucleotide and the peptidic link with the metalloporphyrin precursor was less efficient (cleavage yield = 50%) than **2** with nearly the same total length for the linker (n = 11 and 12 for compounds **4** and **2**, respectively). The two efficient conjugates **1** and **2** have six methylene units between the peptidic link and the 5′-end of oligonucleotide vector, suggesting that the tether between the cleaver entity and the oligonucleotide must be as flexible as possible in order to facilitate interaction of the high-valent metal−oxo species with target. The relative ratio of cleavage products at G_{22}, G_{20}, G_{19}, and T_{18} was the same for compounds **1**−**4**, but the total cleavage yield changed (conjugates **1** and **2** were better cleavers than **3** and **4**). With two methylene units between the 5′-oligonucleotide vector end and the peptidic link, the DNA−metalloporphyrin contacts might be too weak, leading to the self-degradation of the metal−oxo porphyrin rather than to DNA cleavage.

Concerning direct cleavage events (occurring at G_{19} and T_{18} before piperidine treatment) they correspond to a particular interaction of the Mn-cationic porphyrin in the minor groove of ds DNA at three consecutive AT base-pair sequence (5′-AAT_{18} and 5′-AAA_{17} on the 35-mer *tat* target). Within this site of high affinity the metal−oxo porphyrin is able to oxidize the C5′ carbon of the adjacent nucleoside on the 3′-side of the three AT base pairs (Pitié et al., 1992). So if the tethered metalloporphyrin is able to bind in the minor groove of three AT base-pair sequence, then "classical" direct breaks by DNA sugar oxidation should be observed. If not, then the metal−oxo complex abstracts electrons from the easily oxidable guanine residues (Steenken, 1989; Meunier et al., 1994). From CPK models, the tether length of compounds **1**−**4** was too short to allow a good fitting of the cleaving entity within the three AT base-pair sites in the ds zone of oligonucleotide/target duplex. Furthermore, we could observe in the case of compound **1** that G_{19} and T_{18} were not primary cleavage events at low concentrations of $KHSO_5$ (data not shown) but were due to secondary damages. So, the primary damage events were G oxidations, and as the amount of these oxidative damages increased, the C5′ oxidative cleavage at G_{19} and T_{18} as secondary cleavage event was enhanced. The different behavior of compound **5** can be observed, the long tether (n = 21 bonds) allowed relatively more primary cleavage events at G_{19} and T_{18} than G oxidations, compared to the other conjugates of this series. But we were rather disappointed by the spermine linker used for conjugate **5** in terms of yield of cleavage. With triple-helix-forming oligonucleotide linked to the manganese tris(methylpyridiumyl)porphyrin cleaver, we found that the same spermine linker increased the stability of the triplex and consequently enhanced the cleavage yield (Bigey et al., 1995). In the present case, the cleavage efficiency of the spermine-containing conjugate **5** was not as good as expected (yield = 60%). Despite a very long linker (n = 21 bonds) no strong damages were observed at or beyond G_{19} and T_{18}, the main targets of **1** and **2**. But as we already noticed (Pratviel et al., 1995) longer tethers do not increase cleavage efficiency. These experiments suggest that hydrophobic linkers are not an obstacle in the antisense strategy since aliphatic linkers gave better results than the polycationic spermine [for key references on the interactions of spermine derivatives with nucleic acids, see Schmid et al. (1991)].

Influence of Number of Positive Charges of the Porphyrin Ligand on Nuclease Activity of Metalloporphyrin−Oligonucleotide Conjugates. Since manganese tetrakis(4-*N*-meth-

ylpyridiniumyl)porphyrin is the most efficient metalloporphyrin DNA cleaver when activated by monopersulfate (Pitié et al., 1995; Pratviel et al., 1995), we prepared **7**, a conjugate with a tetracationic manganese porphyrin cleaver. This derivative was about ten times more active in the cleavage of the 35-mer *rev* target than the tricationic porphyrin motif (Figures 4 and 5). This enhanced activity might be related to a higher binding affinity of the tetracationic metalloporphyrin for the target nucleic acid and also to a higher reactivity of the high-valent manganese−oxo species due to the electron-withdrawing capacity of the four methylpyridiniumyl substituents at the periphery of the porphyrin ligand. One other advantage of this new cationic manganese porphyrin cleaver is its less tedious preparation via the monoalkylation of the symmetrical tetrapyridylporphyrin.

Influence of the Nature of the Metal Center and of the Activation Mode of the Metalloporphyrin. Expecting an *in vivo* activation mode of these metalloporphyrin−oligonucleotide conjugates similar to that of bleomycin (Pratviel et al., 1989), we compared the nuclease activity of compounds **6** and **8** as a function of the metal (manganese or iron) in both oxidative and aerobic reducing conditions. When activated by $KHSO_5$, the manganese compound **6** was more efficient than its iron analogue **8** in terms of cleavage yield of the degradation of DNA target. The iron conjugate seemed to interact in a different way than **6** with the target since the generated cleavage products of DNA were located at different positions on the 35-mer DNA.

In the case of activation of these manganese porphyrin−oligonucleotide conjugates by an electron source in the presence of O_2, we found that DNA cleavage was highly dependent on the reductant concentration. There was an optimal reductant concentration leading to DNA cleavage: 0.1 mM DTT or glutathione. At smaller or higher concentrations with respect to this optimum, conjugate **6** was inactive. On the other side, the iron conjugate **8** was unable to perform any significant DNA damage when activated by a reducing agent. This phenomenon might be due to a competition between the capacity of the iron−oxo to oxidize the DNA target and its reduction by the large excess of reductant present in the reaction mixture [for kinetic data on these competitive reactions with iron−porphyrin cytochrome P-450 models, see Tabushi et al. (1985)]. The manganese derivative **6** was apparently less sensitive to this phenomenon than the iron conjugate **8**. Taking into account that the iron porphyrin−oligonucleotide conjugate **8** might interact with DNA in a different way than the manganese−oligonucleotide conjugate **6**, this inactivation might be more pronounced for **8** than for **6**.

The important point is the possibility for the manganese−oligonucleotide conjugate **6** to be as efficient as DNA cleaver with an electron source and molecular oxygen than with a peroxide. This key point is determinant for the future possible *in vivo* development of these metalloporphyrin−oligonucleotide conjugates as reactive antisense or antigene oligonucleotides. Due to their higher affinity and reactivity, manganese tetracationic porphyrin−oligonucleotide conjugates are the suitable candidates for studies at the cellular level.

CONCLUSION

Several metalloporphyrin−oligonucleotide conjugates were synthesized by the coupling through an amide bond between a carboxylate arm of a metalloporphyrin and a 5′-amino-oligonucleotide. These different conjugates were then compared on the basis of their DNA cleaving efficiencies in experiments at low DNA cleaver loading (molar ratio of conjugate versus DNA target being 1/1). The most efficient conjugate for the cleavage of a single-stranded DNA target is a manganese tetracationic porphyrin−oligonucleotide conjugate with a linker containing a hexamethylenediamine at the 5′-end of the oligonucleotide vector. The high cleavage efficiency of this conjugate with four positive charges at the periphery of the porphyrin ligand may be related to a higher DNA affinity compared to conjugates based on tris(methylpyridiniumyl)porphyrin derivatives. For the first time, we have been able to obtain an high DNA cleavage activity of a manganese porphyrin−oligonucleotide conjugate when activated by an electron source in the presence of oxygen, with an activation mode similar to that of bleomycin, the antitumor agent able to cleave nuclear DNA of tumor cells.

ACKNOWLEDGMENT

Pr. Jean Bernadou is acknowledged for initiating the preparation of new tetracationic porphyrin precursors from tetrapyridylporphyrin. We thank one referee for detailed comments.

REFERENCES

Bashkin, J. K., Frolova, E. I., & Sampath, U. (1994) *J. Am. Chem. Soc. 116*, 5981−5982.

Bernadou, J., Pratviel, G., Bennis, F., Girardet, M., & Meunier B. (1989) *Biochemistry 28*, 7268−7275.

Bernadou, J., Fabiano, A.-S., Robert, A., & Meunier B. (1994) *J. Am. Chem. Soc. 116*, 9375−9376.

Bigey, P., Pratviel, G., & Meunier, B. (1995a) *J. Chem. Soc., Chem. Commun.*, 181−182.

Bigey, P., Pratviel, G., & Meunier, B. (1995b) *Nucleic Acids Res.23*, 3894−3900.

Bigey, P., Frau, S., Loup, C., Claparols, C., Bernadou, J., & Meunier, B. (1996) *Bull. Soc. Chim. Fr.* (in press).

Burger, R. M., Tian, G., & Drlica, K. (1995) *J. Am. Chem. Soc. 117*, 1167−1168.

Casas, C., St. Jalmes, B., Loup, C., Lacey, C. J., & Meunier B. (1993a) *J. Org. Chem. 58*, 2913−2917.

Casas, C., Lacey, C. J., & Meunier B. (1993b) *Bioconjugate Chem. 4*, 366−371.

Dervan, P. B. (1992) *Nature 359*, 87−88.

Guajardo, R. J., Chavez, F., Farinas, E. T., & Mascharak, P. K. (1995) *J. Am. Chem. Soc. 117*, 3883−3884.

Hall, J., Hüsken, D., Pieles, U., Moser, H. E., & Häner, R. (1994) *Chem. Biol. 1*, 185−190.

Hirao, I., Nishimura, Y., Tagawa, Y.-I., Watanabe, K., & Miura, K.-I. (1992) *Nucleic Acids Res. 20*, 3891−3896.

Hirao, I., Kawai, G., Yoshizawa, S., Nishimura, Y., Ishido, Y., Watanabe, K., & Miura, K.-I. (1994) *Nucleic Acids Res. 22*, 576−582.

Khan, I. M., & Coulson, J. M. (1993) *Nucleic Acids Res. 21*, 2957−2958.

Magda, D., Miller, R. A., Sessler, J. L., & Iverson, B. L. (1994) *J. Am. Chem. Soc. 116*, 7439−7440.

Matsukara, M., Shinozuka, K., Zon, G., Mitsuya, H., Reitz, M., Cohen, J. S., & Broder, S. (1987) *Proc. Natl. Acad. Sci. U.S.A. 84*, 7706−7710.

Matsukara, M., Mitsuya, H., & Broder, S. (1987) in *Prospects for Antisense Nucleic Acid Therapy of Cancer and AIDS* (Wickstrom, E., Ed.) pp 159−178, Wiley-Liss, New York.
Matsumara, K., Endo, M., Komiyama, M. (1994) *J. Chem. Soc., Chem. Commun.,* 2019−2020.
McMurry, T. J., & Groves, J. T. (1986) in *Cytochrome P-450: Structure, Mechanism, and Biochemistry* (Ortiz de Montellano, P. R., Ed.) pp 1−28, Plenum Press, New York.
Mestre, B., Pratviel, G., & Meunier, B. (1995) *Bioconjugate Chem. 6*, 466−472.
Meunier, B. (1992) *Chem. Rev. 92*, 1411−1456.
Meunier, B., Pratviel, G., & Bernadou, J. (1994) *Bull. Soc. Chim. Fr. 131*, 933−943.
Pitié, M., Pratviel, G., Bernadou, J., & Meunier, B. (1992) *Proc. Natl. Acad. Sci. U.S.A. 89*, 3967−3971.
Pitié, M., Casas, C., Lacey, C. J., Pratviel, G., Bernadou, J., & Meunier, B. (1993) *Ang. Chem., Int. Ed. Engl. 32*, 557−559.
Pitié, M., Bernadou, J., & Meunier, B. (1995) *J. Am. Chem. Soc. 117*, 2935−2936.
Poddevin, B., Meguenni, S., Elias, I., Vasseur, M., & Blumenfeld M. (1994) *Antisens Res., & Dev. 4*, 147−154.
Pratviel, G., Bernadou, J., & Meunier, B. (1989) *Biochem. Pharmacol. 38*, 133−140.
Pratviel, G., Duarte, V., Bernadou, J., & Meunier, B. (1993a) *J. Am. Chem. Soc. 115*, 7939−7943.
Pratviel, G., Pitié, M., Périgaud, C., Gosselin, G., Bernadou, J., & Meunier, B. (1993b) *J. Chem. Soc., Chem. Commun.*, 149−151.
Pratviel, G., Bigey, P., Bernadou, J., & Meunier, B. (1995) in *Genetic Response to Metals* (Sarkar, B., Ed.) pp 153−171, Marcel Dekker, New York.
Sam, J. W., Tang, X. -J., & Peisach, J. (1994) *J. Am. Chem. Soc. 116*, 5250−5256.
Schmid, N., & Behr, J. P. (1991) *Biochemistry 30*, 4357−4361.
Sigman, D. S., Bruice, T. W., Mazumder, A., & Sutton, C. L. (1993) *Acc. Chem. Res. 26*, 98−104.
Steenken, S. (1989) *Chem. Rev. 89*, 503−520.
Tabushi, I., Kodera, M., & Yokoyama, M. (1985) *J. Am. Chem. Soc. 107*, 4466−4473.
Wachter, L., Jablonski, J. A., & Ramachandran, K. L. (1986) *Nucleic Acids Res. 14*, 7985−7994.
Wain-Hobson, S., Sonigo, P., Danos, O., Cole, S., & Alizon, M. (1985) *Cell 40*, 9−17.
Ward, B., Skorobogaty, A., & Dabrowiak, J. C. (1986) *Biochemistry 25*, 6875−6883.

BI9530402